ADVANCED MATERIALS

Research News

Evaporation-Induced Self-Assembly: Nanostructures Made Easy**

By C. Jeffrey Brinker,* Yunfeng Lu, Alan Sellinger, and Hongyou Fan

1. Introduction

As we look toward the next millennium, we envision new technologies based on nanoscale machines and devices. Key to the realization of this nanotech world are simple, efficient methods of organizing materials (molecules, molecular clusters, polymers, or, generally speaking, building blocks) into precise, predetermined nanostructures that can be preserved in a robust engineering form. Marine organisms like diatoms and radiolaria provide us with many examples of intricately organized architectures preserved in silica or calcium carbonate. Such natural microstructures are formed by biomineralization,[1] a templated self-assembly process in which preorganized organic surfaces regulate the nucleation, growth, morphology and orientation of inorganic crystals. To date, a variety of synthetic pathways that mimic aspects of biomineralization have been explored to prepare patterned ceramic materials.[2–4] In an early attempt to achieve antigen/antibody selectivity in a porous adsorbent, Dickey[5] prepared silica gels in the presence of the target molecule to be adsorbed (in this case methyl orange). After methyl orange extraction, the resulting templated silicas showed preferential selectivity for methyl orange over its alkyl orange homologues. In the 1960s researchers at the Mobil Oil Corporation[6] used alkylammonium ions as templates to control the pore size, shape and periodicity of zeolites, crystalline solids that define 1-, 2-, or 3-dimensional (1-, 2-, or 3-D, respectively) networks of microporous channels. More recently Kresge and colleagues at Mobil[7] used longer-chain alkylammonium ions in an attempt to increase the maximum pore size of zeolites beyond ~1.2 nm. They observed honeycomb-like arrays of ~4 nm pores and, based on analogies with hexagonal liquid-crystalline systems, proposed a supramolecular liquid-crystalline templating mechanism.

Although excellent progress has been made in the preparation of a wide variety of patterned ceramic materials,[8] current synthetic methods have several inherent drawbacks from the standpoint of nanotechnology: First, most templating procedures are conducted in time-consuming batch operations often employing hydrothermal processing conditions. Second, the resultant products are typically ill-defined powders, precluding their general use in thin film technologies. Third, procedures developed to date are often limited to forming patterns of pores. For many envisioned nanotechnologies, it would be desirable to create patterned nanocomposites consisting of periodic arrangements of two or more dissimilar materials. This article summarizes a simple evaporation-induced self-assembly (EISA) process, that enables the rapid production of patterned porous or nanocomposite materials in the form of films, fibers, or powders.

2. Self-Assembly

A general definition of self-assembly is the spontaneous organization of materials through noncovalent interactions (hydrogen bonding, Van der Waals forces, electrostatic forces, π–π interactions, etc.) with no external intervention. Self-assembly typically employs asymmetric molecules that are pre-programmed to organize into well-defined supramolecular assemblies. Most common are amphiphilic surfactant molecules or polymers composed of hydrophobic and hydrophilic parts. In aqueous solution above the critical micelle concentration (cmc), surfactants assemble into micelles, spherical or cylindrical structures that maintain the hydrophilic parts of the surfactant in contact with water

[*] Dr. C. J. Brinker, Dr. Y. Lu
Sandia National Laboratory
Direct Fabrication Department 1831
Albuquerque, NM 87185 (USA)
Dr. A. Sellinger
Canon Research Center America, Inc.
4009 Miranda Avenue
Palo Alto CA, 94304 (USA)
Dr. C. J. Brinker, Dr. H. Fan
University of New Mexico Center for Microengineered Materials
Advanced Materials Lab
1001 University Blvd. SE, Albuquerque, NM 87106 (USA)

[**] This work was funded by grants from the Department of Energy Basic Energy Sciences Program, Sandias Laboratory-Directed Research and Development Program, and the University of New Mexico/NSF Center for Microengineered Materials. The authors thank Tim Ward, Rahul Ganguli, Alan Hurd, Frank van Swol, and John Shelnutt for useful discussions and Kelley Burns for editorial assistance. Sandia is a multiprogram laboratory operated by Sandia Corporation, a Lockheed Martin Company, for the United States Department of Energy under Contract DE-AC04-94AL85000.

  0935-9648/99/0705-0579 $ 17.50+.50/0

while shielding the hydrophobic parts within the micellar interior (see Fig. 1). Further increases in surfactant concentration result in the self-organization of micelles into periodic hexagonal, cubic, or lamellar mesophases (Fig. 1).

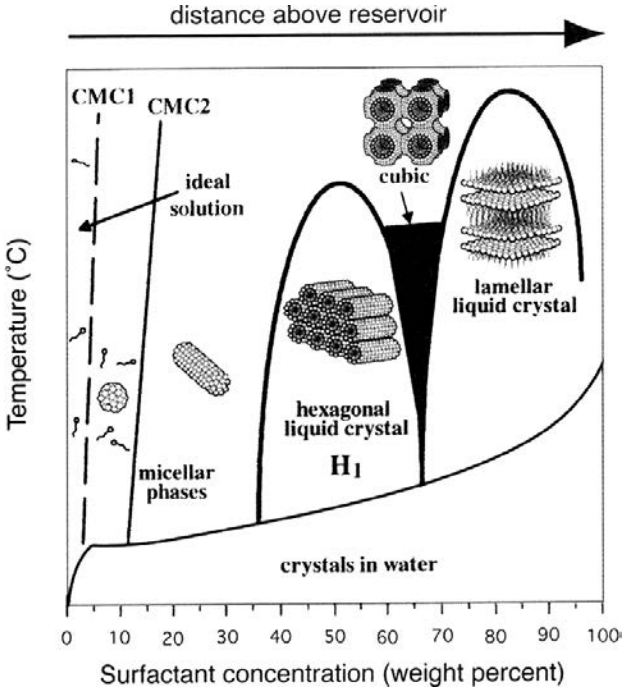

Fig. 1. Schematic phase diagram for CTAB in water. Arrow denotes evaporation-driven pathway during dip-coating, aerosol processing, etc. Adapted from Raman et al. [33].

Obviously such detergent mesophases do not themselves represent robust engineering materials suitable for nanotechnologies. However in 1992 Mobil researchers[7] discovered that surfactant self-assembly conducted in aqueous solutions of soluble silica species results in spontaneous co-assembly of silica–surfactant mesophases. Surfactant removal creates periodic mesoporous solids, essentially silica fossils of the liquid-crystalline assembly. Over the last eight years, this pioneering work has been extended to produce a wide compositional range of mesoporous solids, and, using a variety of surfactants, the pore sizes have been varied in the approximate range, 1 nm to over 10 nm.[9–13] Despite excellent control of pore size, early mesoporous materials were made in the form of powders, precluding their use in thin film applications like membranes, low dielectric constant interlayers, and optical sensors. Stable, supported, mesoporous silica films were reported in 1996.[2,14,15] Typically, substrates were introduced into silica/surfactant/solvent systems used to prepare bulk hexagonal mesophases (initial surfactant concentrations $c_0 >$ cmc). Under these conditions, hexagonal silica–surfactant mesophases are nucleated on the substrate with pores oriented parallel to the substrate surface. Growth and coalescence over a period of hours to weeks resulted in continuous but macroscopically inhomogeneous films characterized by granular textures on micrometer-length scales.

3. Evaporation-Induced Self-Assembly

Consideration of Figure 1 in the context of sol-gel dip-coating suggests an alternative route to the formation of thin film mesophases. Beginning with a homogeneous solution of soluble silica and surfactant prepared in ethanol/water solvent with $c_o \ll$ cmc, preferential evaporation of ethanol concentrates the depositing film in water and nonvolatile surfactant and silica species (Fig. 2). The progressively increasing surfactant concentration drives self-assembly of silica–surfactant micelles and their further organization into liquid-crystalline mesophases.[16–18] Pre-existing, incipient silica–surfactant mesostructures (which exist at solid–liquid and liquid–vapor interfaces at $c <$ cmc) serve to nucleate and orient mesophase development.[2,19] The result is rapid formation of thin film mesophases that are highly oriented with respect to the substrate surface. Through variation of the initial alcohol/water/surfactant mole ratio it is possible to follow different trajectories in composition space (see Fig. 2b) and to arrive at different final mesostructures. For example, using cetyltrimethylammonium bromide (CTAB), we demonstrated the formation of 1-D hexagonal, cubic, 3-D hexagonal and lamellar silica–surfactant mesophases.[15–17] Transmission electron micrographs of representative cubic thin film mesophases are shown in Figure 3. Such cubic mesophases are crucial for applications like membranes and sensors because they guarantee pore accessibility and through-film pore connectivity.

The dip-coating scheme depicted in Figure 2 represents a rapid (~10 s), dynamic self-assembly process conducted in a rather steep concentration gradient. Its steady, continuous nature promotes continuous accretion of micellar or perhaps liquid-crystalline species onto interfacially organized mesostructures. Large, liquid-crystalline domains grow progressively inward from the solid–liquid and liquid–vapor interfaces (with increasing distance above the reservoir surface, Fig. 2). Deposited films are optically transparent and completely featureless on the micrometer-length scale.

Essential to our ability to rapidly organize thin film mesophases is suppression of inorganic polymerization during the coating operation. For silicates this is achieved under acidic conditions at a hydronium ion concentration corresponding closely to the isoelectric point of colloidal silica ($[H_3O^+] \sim 0.01$).[20] By first turning off siloxane condensation, we allow cooperative silica–surfactant self-assembly to proceed unimpeded, and the resulting as-deposited films exhibit liquid-crystalline (semi-solid) behavior. Subsequent aging, exposure to acid or base catalysts, or thermal treatment can solidify the silica skeleton, thereby locking in the desired mesostructure.

Evidence for the liquid-crystalline nature of as-deposited films is several-fold: First, using a cantilever beam technique we showed there to be dramatically less tensile stress developed during mesophase thin film deposition (5–10 MPa) compared to deposition of the same silica sol prepared without surfactants (~200 MPa). This virtual

  0935-9648/99/0705-0580 $ 17.50+.50/0

ADVANCED MATERIALS

a)

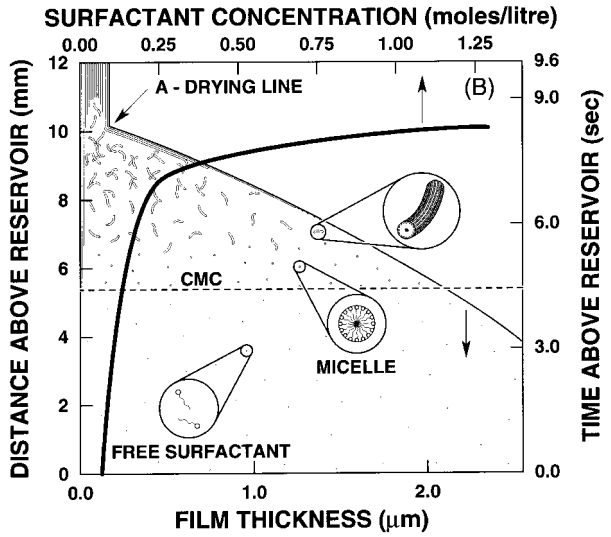

b)

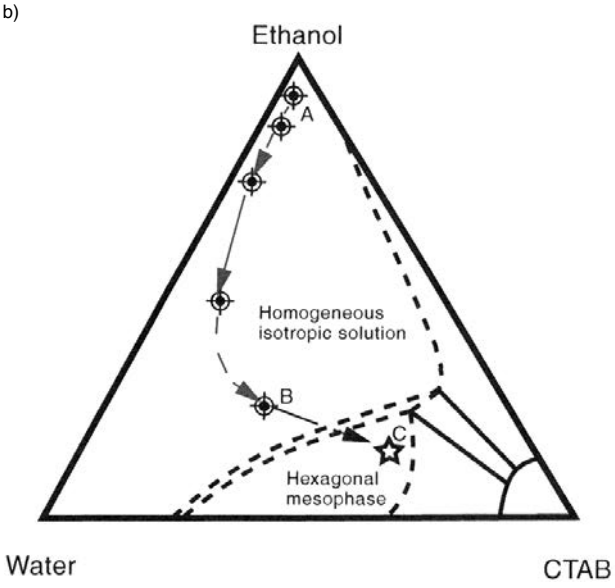

Fig. 2. a) Steady-state film thinning profile established during dip-coating of a complex fluid comprising soluble silica, surfactant, alcohol, and water. Initial surfactant concentration $c_o \ll$ cmc. Surfactant concentration increases with distance above the reservoir surface. Adapted [16]. b) Approximate trajectory taken in ethanol/water/CTAB phase space during dip-coating. Point A corresponds to the initial composition of entrained solution, Point B is near the drying line, and Point C corresponds to the dried film. Pathway calculated by combining results of in situ probe experiments [34] and imaging ellipsometry [35], and superimposing data onto the experimental phase diagram determined by Fontell et al. [36].

absence of drying stress suggests that the film completely dries prior to solidification (i.e., as-deposited films are not solidified). Second, we have shown that as-deposited mesophase films can be transformed to completely different mesophases (e.g., lamellar → cubic).[16] Third, the as-deposited films exhibit self-healing tendencies. These combined liquid-crystalline characteristics make the EISA process robust yet versatile. Advantages of using liquid-crystalline intermediates as templates in the generalized synthesis of mesoporous materials were recently reported by Göltner and Antonietti.[21]

4. Sea Shells

The mollusk shell has long been heralded as the holy grail of natural materials design and construction. Its microlaminated architecture composed of alternating layers of aragonite (a crystalline form of calcium carbonate) and a rubbery biopolymer has evolved over millions of years to simultaneously provide strength, hardness, and toughness to a light weight material. For example abalone nacre composed of only 1 wt.-% polymer is twice as hard, and 1000 times tougher than its constituent phases.[22] Key to the desirable mechanical properties of such natural laminates is the capacity of the soft organic layers to absorb energy through deformation and the presence of multiple hard–soft interfaces that serve to deflect cracks, requiring continued crack initiation to sustain crack propagation.

The remarkable combination of properties of natural biocomposites has inspired chemists and materials scientists to devise synthetic so-called biomimetic pathways for their construction. There exist two general biomimetic approaches: The first involves directly mimicking a biological process. The second approach, sometimes referred to as bio-inspired, attempts to imbed natural features in a synthetic material but uses nonbiological processing schemes and often completely different materials combinations. For example, organic/inorganic nanocomposites have been prepared using layer-by-layer approaches[23,24] in which anionic and cationic precursors (e.g., clays and polyelectrolytes) are sequentially deposited on the substrate surface. Obviously many successive dip-adsorb-wash-dip cycles are required to construct composite coatings in this manner, and the resulting films are generally glued together with electrostatic rather than covalent bonds.

5. Nanocomposite Self-Assembly

Nanocomposite self-assembly[25] represents an extension of the EISA process described above. Using the generic detergent phase diagram shown in Figure 4 as a conceptual guide, we can consider as oil a wide variety of hydrophobic, organic precursors and reagents (monomers, crosslinkers, oligomers, functionalized polymers, initiators, etc.). In a process not so unlike washing dishes, we use micelle formation to spatially separate and organize organic precursors (sequestered within the hydrophobic micellar interiors) and inorganic precursors (organized around the hydrophilic micellar exteriors). Further self-organization of micelles into periodic hexagonal, cubic, or lamellar mesophases simultaneously positions both the organic and inorganic precursors into precise 3-D arrangements. Combined organic/inorganic polymerization locks in the nanocomposite architecture and covalently bonds the organic/

  0935-9648/99/0705-0581 $ 17.50+.50/0

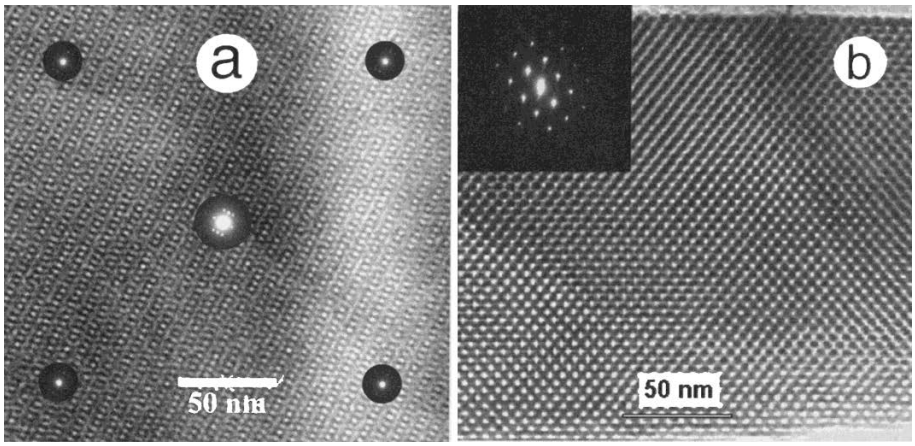

Fig. 3. Representative TEM micrographs of cubic thin film mesophases. a) TEM plan view of calcined film prepared from CTAB, showing large [210]-oriented domain of cubic mesophase (adapted [16]). b) Cross-sectional TEM of calcined cubic film formed from the nonionic surfactant, Brij-56 [38].

inorganic interface. The beauty of this approach is its simplicity and efficiency: if we seek to prepare laminated organic/inorganic composites, many hundreds of alternating organic/inorganic layers can be assembled in seconds.

As described above for thin film mesophases, nanocomposite self-assembly is driven by evaporation during film deposition (Fig. 5a).[25] We begin with a homogeneous solution of soluble silicates, surfactant, organic monomers, and photo or thermal initiators prepared in ethanol/water solvent with c_o < cmc. During coating, preferential evaporation of ethanol (used initially to solubilize the organic precursors and homogenize the solution), progressively enriches the concentrations of water, HCl and the nonvolatile solution constituents within the depositing film. As confirmed by optical probe studies,[16] the increasing concentrations of surfactant and water cause the surfactant concentration to exceed the cmc, resulting in micelle formation and concurrent partitioning of the organic precursors and initiators into the micellar interiors and the inorganic precursors surrounding the micellar exteriors. Continued evaporation promotes co-assembly of these species into liquid-crystalline mesophases, thereby simultaneously organizing both the organic and inorganic precursors into the desired laminated form (Fig. 5b). Photo or thermally induced polymerization of the organic monomers and continued inorganic polymerization complete the composite assembly process (Fig. 5c). Figure 6 shows a representative transmission electron microscopy (TEM) cross-section of a poly (dodecylmethacrylate)/silica nanolaminate coating composed of over 150 alternating organic/inorganic layers formed in a single step. ^{13}C and ^{29}Si solid state nuclear magnetic

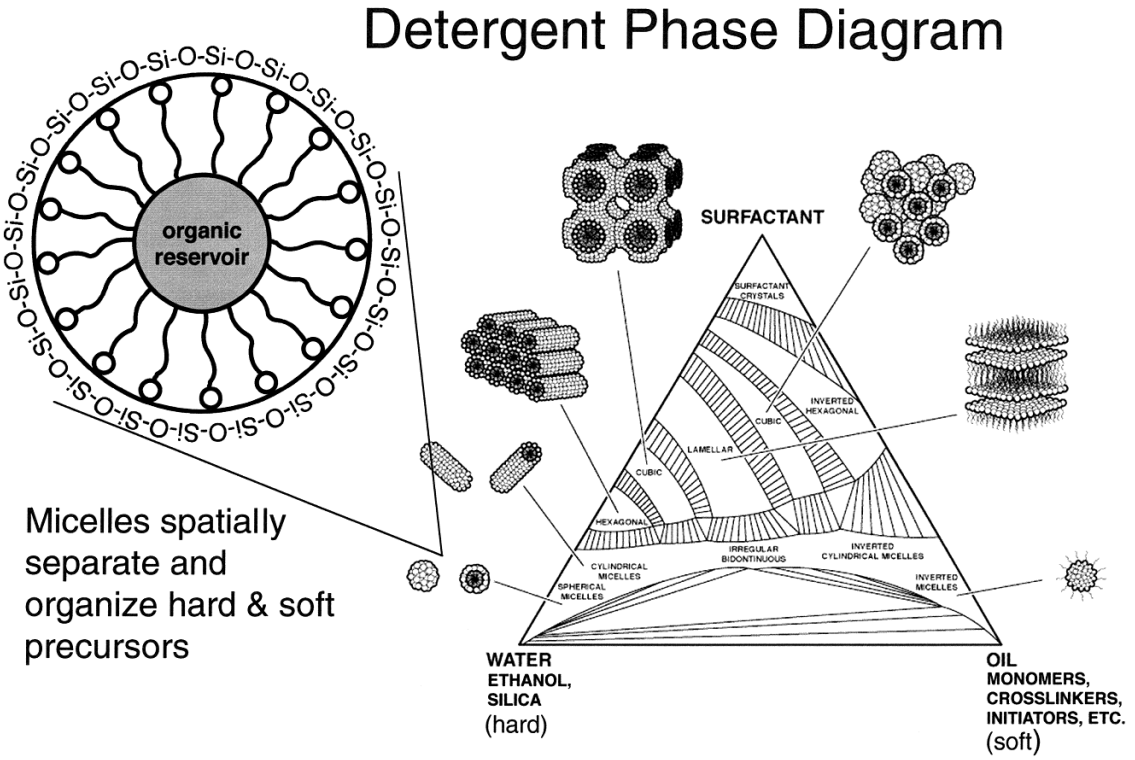

Fig. 4. Schematic detergent (surfactant–oil–water) phase diagram. With the introduction of hydrophobic organic (or generally soft) precursors and hydrophilic inorganic (or generally hard) precursors, organic constituents partition within the hydrophobic micellar interiors, while inorganic constituents are organized around the micellar exteriors. Evaporation promotes further self-assembly into liquid-crystalline mesophases, simultaneously organizing organic and inorganic precursors into nanocomposite architectures.

  0935-9648/99/0705-0582 $ 17.50+.50/0

ADVANCED MATERIALS

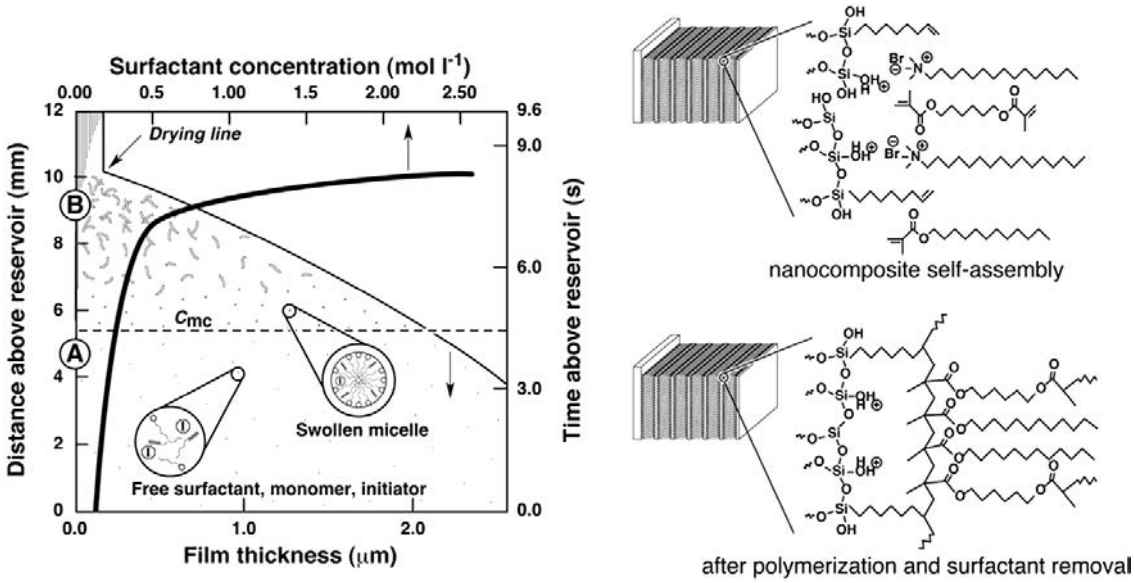

Fig. 5. a) Schematic illustration of self-assembly of organic–inorganic nanolaminates during dip-coating. Evaporation induces micelle formation and concurrent incorporation of organic precursors into micellar interiors. Further evaporation drives continuous accretion of micellar species onto interfacially-organized lamellar layers, simultaneously organizing the organic and inorganic precursors into the desired nanolaminated form. b) Hypothetical arrangement of surfactant, monomer, crosslinker, and initiator (I) adjacent to an oligomeric silica layer. c) Hypothetical structure of covalently bonded silica/poly(dodecylmethacrylate) nanocomposite (adapted [25]).

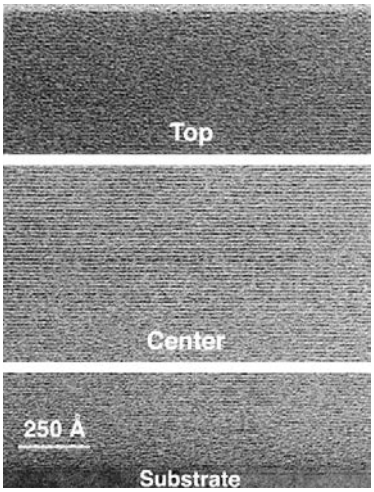

Fig. 6. TEM cross-section of ~500 nm thick nanocomposite film showing *c*-axis oriented nanolaminate structure. Shown are representative sections of the coating in the central region and regions adjacent to the substrate and vapor surfaces. Coating contains over 150 organic–inorganic layers formed in a single dip-coating step [25].

resonance spectroscopy (NMR) was used to confirm both methacrylate and siloxane condensation as well as covalent bonding of the methacrylate/siloxane interface (via an octenyltrimethoxysilane coupling agent).[25]

6. Aerosol-Assisted Self-Assembly of Nanoparticles

Nanostructured particles exhibiting well-defined pore sizes and pore connectivities (1, 2, or 3-D) are of interest for catalysis, chromatography, controlled release, low dielectric constant fillers, and custom engineered pigments and optical hosts.[26,27] Based on the above discussion, it seems obvious to consider evaporation-induced self-assembly of liquid droplets as a means to create such particles. Starting with an aerosol dispersion of the same precursor solutions used to create mesoporous or nanocomposite films, we expect solvent evaporation to create a radial gradient of surfactant concentration within each droplet that steepens in time[28] and maintains a maximum concentration at the droplet surface. In this situation, the surfactant cmc is exceeded first at the surface of the droplet, and, as evaporation proceeds, cmc is progressively exceeded throughout the droplet. This surfactant enrichment induces silica–surfactant self-assembly into micelles and further organization into liquid-crystalline mesophases. The radial concentration gradient and presence of the liquid–vapor interface (which serves as a nucleating surface)[19] causes ordered silica–surfactant liquid-crystalline (LC) domains to grow radially inward, rather than outward from a seed.[29] As in the case of films, a key to the formation of solid, completely ordered particles is maintenance of a liquid or liquid-crystalline state throughout the course of the EISA process. Premature solidification would result in the formation of hollow particles[19] and inhibit orderly self-assembly that must proceed with continual restructuring of the evolving silica–surfactant mesophase in order to accommodate drying shrinkage.

Using the aerosol reactor apparatus depicted in Figure 7, we recently demonstrated EISA of aerosol droplets. Figures 8a–c show TEM micrographs of representative mesoporous particles prepared with various surfactant templates (cationic, nonionic, block copolymer). For these particles, the furnace was operated at 400 °C and the volumetric flow rate of the carrier gas was 2.6 standard liters

  0935-9648/99/0705-0583 $ 17.50+.50/0

of N_2/min, establishing laminar flow conditions throughout the reactor (Reynolds number = 75). In a continuous, ~6 second process, the aerosol particles were dried, heated, and collected. If the furnace was not operated, the dried aerosol particles coalesced on the collection surface to form a completely ordered thin film mesophase (Fig. 8d). The ability of nominally dry particles to coalesce into a continuous film provides further evidence of the semi-solid nature of ordered silica–surfactant mesophases and their inherent self-healing characteristics.

We note that the curvature of the particle surface profoundly influences mesostructure development. This is evident in the comparison of CTAB-templated particles (e.g., Fig. 8a) and corresponding mesostructured films formed on flat substrates by EISA during dip-coating.[16] Unlike films, which have flat liquid–vapor interfaces and show a progressive change in mesostructure (disordered → hexagonal → cubic → lamellar) with increasing surfactant concentration,[16] particles prepared with comparable CTAB concentrations exhibit only disordered or hexagonal mesophases. We conclude that, since the liquid–vapor interface serves as a nucleating surface for liquid crystal growth, the high curvature imposed by this interface alters the generally observed relationship between surfactant packing parameter and resulting mesostructure.[30] Although CTAB commonly forms lamellar mesophases in bulk and thin film samples,[7,18] apparently it cannot pack into a cone truncated by surfaces of high and opposite curvature needed to direct the corresponding vesicular mesostructure of nanoparticles (nested concentric spheres; see for example Fig. 8c).

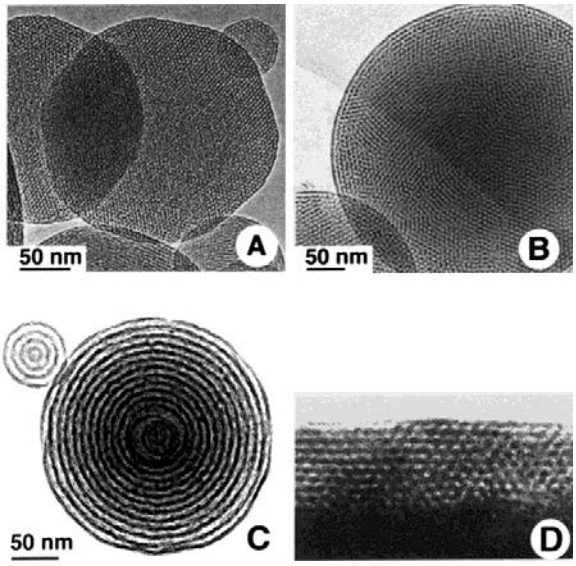

Fig. 8. TEM micrographs of aerosol-generated particles and an aerosol-deposited thin film. a) Faceted, calcined particles exhibiting 1-D hexagonal mesophase, prepared using CTAB. b) Calcined particles exhibiting cubic mesophase, prepared from the nonionic surfactant Brij-58. c) Calcined particles exhibiting vesicular mesophase, prepared from the ethylene oxide/propylene oxide/ethylene oxide tri-block copolymer P123. d) Cross-section of film deposited on silicon substrate by coalescence of aerosol droplets. Precursor solution prepared with P123 (identical to that in Fig. 8c). Film deposition was conducted without operation of the furnace. (Adapted [37]).

7. Future Directions

Evaporation-induced self-assembly can be combined readily with micrometer-scale film patterning strategies such as microcontact printing,[31] direct writing, or lithography. In addition, using organoalkoxysilane precursors ($R'Si(OR)_3$, where R′ represents an organic ligand) or organic additives such as dye molecules, it is possible to modify extensively local (molecular-scale) chemistry and structure.[32] In combination, these attributes should provide a convenient pathway to the formation of functional hierarchical devices. As an example, Figure 9 shows a macro-patterned, meso-

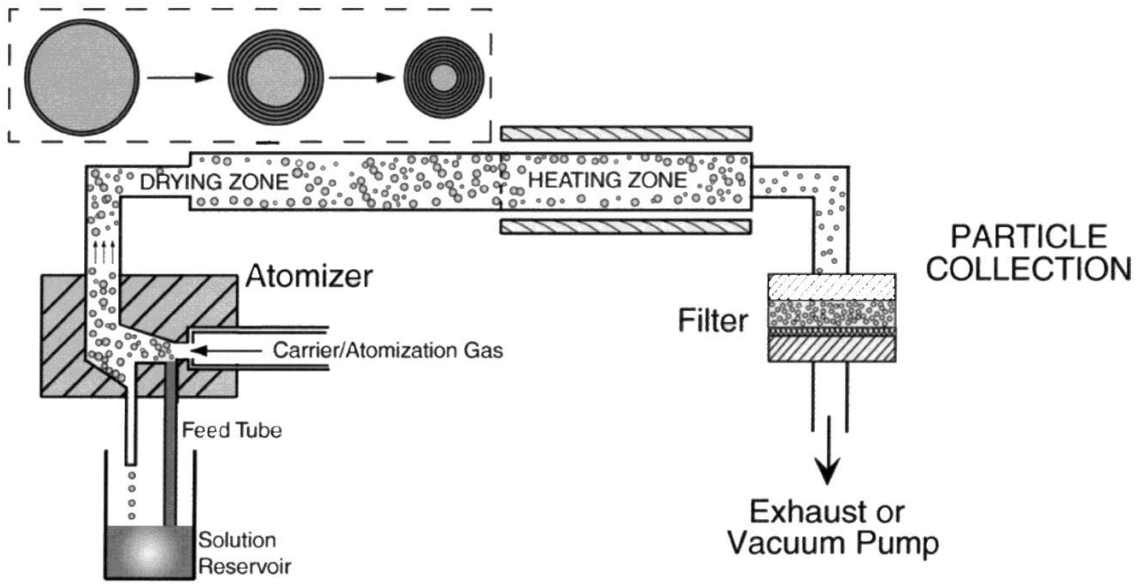

Fig. 7. Schematic of aerosol reactor (adapted [37]).

0935-9648/99/0705-0584 $ 17.50+.50/0

ADVANCED MATERIALS

porous film containing the fluorescent dye rhodamine. The film was made in a single step by dip-coating on a microcontact-printed substrate.

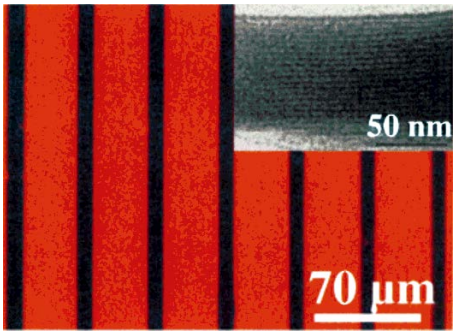

Fig. 9. Optical fluorescence micrograph of patterned rhodamine-containing thin film mesophase formed by dip-coating on an SAM-patterned substrate prepared by microcontact printing. Inset: TEM micrograph of rhodamine containing 1-dimensional hexagonal mesostructure[38].

Having demonstrated an efficient composite self-assembly process to make nanolaminated structures that mimic shell, we can consider alternate composite architectures (e.g., those based on hexagonal or cubic mesophases) along with an unlimited number of binary materials combinations. As such, nanocomposite self-assembly can be considered an efficient structure-generating approach for nanocomposite materials discovery. By variation of composite mesostructure, materials combinations, interfacial chemistry, and characteristic (confining) dimensions, we should expect to discover new materials properties.

Finally we can envision the aerosol route as a simple means to capture polymers, particles, drugs, and even bioactive species within a highly structured nanocontainer. By variation of the self-assembled mesostructure, the accessibility and diffusivity of the guest species could be controlled closely. We wonder if, by introducing a mixture of guest species, the differential curvature of each succeeding layer of the vesicular mesophase would selectively position different species at different radial positions. This approach could lead to radially-graded hierarchical materials that might facilitate vectorial energy transfer as in photosynthesis centers.

[1] S. Mann, *Nature* **1993**, *365*, 499.
[2] I. Aksay, M. Trau, S. Manne, I. Honma, N. Yao, L. Zhou, P. Fenter, P. Eisenberger, S. Gruner, *Science* **1996**, *273*, 892.
[3] A. Heuer, D. Fink, V. Laraia, J. Arias, P. Calvert, K. Kendall, G. Messing, J. Blackwell, P. Rieke, D. Thompson, A. Wheeler, A. Veis, A. Caplan, *Science* **1992**, *255*, 1098.
[4] G. A. Ozin, *Acc. Chem. Res.* **1996**, A–K.
[5] F. H. Dickey, *Proc. Natl. Acad. Sci.* **1949**, *35*, 227.
[6] R. M. Barrer, P. J. Denny, *J. Chem. Soc.* **1961**, 971.
[7] C. Kresge, M. Leonowicz, W. Roth, C. Vartuli, J. Beck, *Nature* **1992**, *359*, 710.
[8] S. Mann, G. A. Ozin, *Nature* **1996**, *382*, 313.
[9] Q. Huo, D. Margolese, U. Ciesla, P. Feng, T. G. Gier, P. Sieger, R. Leon, P. M. Petroff, F. Schuth, G. Stucky, *Nature* **1994**, *368*, 317.
[10] A. Firouzi, D. Kumar, L. M. Bull, T. Besier, P. Sieger, Q. Huo, S. A. Walker, J. A. Zasadzinski, C. Glinka, J. Nicol, D. Margolese, G. D. Stucky, B. F. Chmelka, *Science* **1995**, *267*, 1138.
[11] P. T. Tanev, T. J. Pinnavaia, *Science* **1995**, *267*, 865.
[12] D. M. Antonelli, J. Y. Ying, *Angew. Chem. Int. Ed. Engl.* **1995**, *34*, 2014.
[13] D. Zhao, J. Feng, Q. Huo, N. Nelosh, G. Fredrickson, B. Chmelka, G. D. Stucky, *Science* **1998**, *279*, 548.
[14] H. Yang, A. Kuperman, N. Coombs, S. Mamiche-Afara, G. A. Ozin, *Nature* **1996**, *379*, 703.
[15] M. Ogawa, *Chem. Commun.* **1996**, 1149.
[16] Y. Lu, R. Ganguli, C. Drewien, M. Anderson, C. Brinker, W. Gong, Y. Guo, H. Soyez, B. Dunn, M. Huang, J. Zink, *Nature* **1997**, *389*, 364.
[17] P. J. Bruinsma, A. Y. Kim, J. Liu, S. Baskaran, *Chem. Mater.* **1997**, *9*, 2507.
[18] M. Ogawa, *J. Am. Chem. Soc.* **1994**, *116*, 7941.
[19] H. Yang, N. Coombs, I. Sokolov, G. A. Ozin, *Nature* **1996**, *381*, 589.
[20] C. J. Brinker, G. W. Scherer, *Sol-Gel Science*, Academic, **1990**.
[21] C. G. Göltner, M. Antonietti, *Adv. Mater.* **1997**, *9*, 431.
[22] A. Jackson, J. Vincent, R. Turner, in *Proceedings of the Royal Society of London Series B–Biological Sciences*, Royal Society of Chemistry, London **1988**, p. 415.
[23] S. Keller, H. Kim, T. Mallouk, *J. Am. Chem. Soc.* **1994**, *116*, 8817.
[24] E. Kleinfeld, G. Ferguson, *Science* **1994**, *265*, 370.
[25] A. Sellinger, P. M. Weiss, A. Nguyen, Y. Lu, R. A. Assink, W. Gong, C. J. Brinker, *Nature* **1998**, *394*, 256.
[26] Q. Huo, J. Feng, F. Schuth, G. D. Stucky, *Chem. Mater.* **1997**, *9*, 14.
[27] G. A. Ozin, *Adv. Mater.* **1992**, *4*, 612.
[28] G. V. Jayanthi, S. C. Zhang, G. L. Messing, *Aerosol Sci. Tech.* **1993**, *19*, 478.
[29] H. Yang, N. Coombs, G. A. Ozin, *Nature* **1997**, *386*, 692.
[30] J. Israelachvili, *Intermolecular and Surface Forces*, Academic, San Diego, CA **1992**.
[31] N. Jeon, K. Finnie, K. Branshaw, R. Nuzzo, *Langmuir* **1997**, *13*, 3382.
[32] S. Burkett, S. Sims, S. Mann, *Chem. Commun.* **1996**, *11*, 1367.
[33] N. Raman, M. Anderson, C. Brinker, *Chem. Mater.* **1996**, *8*, 1682.
[34] F. Nishida, J. McKiernan, B. Dunn, J. Zink, C. Brinker, A. Hurd, *J. Am. Ceram. Soc.* **1995**, *78*, 1640.
[35] R. Ganguli, *Mesoporous Thin Silica Films Created by the Templating of CTAB Mesophases*, Masters in Chemical & Nuclear Engineering Albuquerque University of New Mexico **1977**.
[36] K. Fontell, A. Khan, B. Lindstrom, D. Maciejewska, S. Puang-Ngern, *Colloid Polym. Sci.* **1991**, *269*, p 727.
[37] Y. Lu, H. Fan, A. Stump, T. L. Ward, T. Rieker, C. J. Brinker, *Nature* **1999**, *398*, 223.
[38] H. Fan et al., unpublished results.

  0935-9648/99/0705-0585 $ 17.50+.50/0